Fermi National Accelerator Laboratory

FERMILAB-Pub-95/038-E

CDF

Properties of High-Mass Multijet Events at the Fermilab Proton-Antiproton Collider

F. Abe et al.
The CDF Collaboration

Fermi National Accelerator Laboratory
P.O. Box 500, Batavia, Illinois 60510

March 1995

Submitted to *Physical Review Letters*

Operated by Universities Research Association Inc. under Contract No. DE-AC02-76CHO3000 with the United States Department of Energy

Disclaimer

FERMILAB-PUB-95/038-E
CDF/PUB/JET/PUBLIC/2957

Properties of High-Mass Multijet Events at the Fermilab Proton-Antiproton Collider

F. Abe,[13] M. G. Albrow,[7] S. R. Amendolia,[23] D. Amidei,[16] J. Antos,[28] C. Anway-Wiese,[4] G. Apollinari,[26] H. Areti,[7] M. Atac,[7] P. Auchincloss,[25] F. Azfar,[21] P. Azzi,[20] N. Bacchetta,[18] W. Badgett,[16] M. W. Bailey,[18] J. Bao,[35] P. de Barbaro,[25] A. Barbaro-Galtieri,[14] V. E. Barnes,[24] B. A. Barnett,[12] P. Bartalini,[23] G. Bauer,[15] T. Baumann,[9] F. Bedeschi,[23] S. Behrends,[3] S. Belforte,[23] G. Bellettini,[23] J. Bellinger,[34] D. Benjamin,[31] J. Benlloch,[15] J. Bensinger,[3] D. Benton,[21] A. Beretvas,[7] J. P. Berge,[7] S. Bertolucci,[8] A. Bhatti,[26] K. Biery,[11] M. Binkley,[7] F. Bird,[29] D. Bisello,[20] R. E. Blair,[1] C. Blocker,[3] A. Bodek,[25] W. Bokhari,[15] V. Bolognesi,[23] D. Bortoletto,[24] C. Boswell,[12] T. Boulos,[14] G. Brandenburg,[9] C. Bromberg,[17] E. Buckley-Geer,[7] H. S. Budd,[25] K. Burkett,[16] G. Busetto,[20] A. Byon-Wagner,[7] K. L. Byrum,[1] J. Cammerata,[12] C. Campagnari,[7] M. Campbell,[16] A. Caner,[7] W. Carithers,[14] D. Carlsmith,[34] A. Castro,[20] Y. Cen,[21] F. Cervelli,[23] H. Y. Chao,[28] J. Chapman,[16] M.-T. Cheng,[28] G. Chiarelli,[8] T. Chikamatsu,[32] C. N. Chiou,[28] S. Cihangir,[7] A. G. Clark,[23] M. Cobal,[23] M. Contreras,[5] J. Conway,[27] J. Cooper,[7] M. Cordelli,[8] C. Couyoumtzelis,[23] D. Crane,[1] J. D. Cunningham,[3] T. Daniels,[15] F. DeJongh,[7] S. Delchamps,[7] S. Dell'Agnello,[23] M. Dell'Orso,[23] L. Demortier,[26] B. Denby,[23] M. Deninno,[2] P. F. Derwent,[16] T. Devlin,[27] M. Dickson,[25] J. R. Dittmann,[6] S. Donati,[23] R. B. Drucker,[14] A. Dunn,[16] K. Einsweiler,[14] J. E. Elias,[7] R. Ely,[14] E. Engels, Jr.,[22] S. Eno,[5] D. Errede,[10] S. Errede,[10] Q. Fan,[25] B. Farhat,[15] I. Fiori,[2] B. Flaugher,[7] G. W. Foster,[7] M. Franklin,[9] M. Frautschi,[18] J. Freeman,[7] J. Friedman,[15] H. Frisch,[5] A. Fry,[29] T. A. Fuess,[1] Y. Fukui,[13] S. Funaki,[32] G. Gagliardi,[23] S. Galeotti,[23] M. Gallinaro,[20] A. F. Garfinkel,[24] S. Geer,[7] D. W. Gerdes,[16] P. Giannetti,[23] N. Giokaris,[26] P. Giromini,[8] L. Gladney,[21] D. Glenzinski,[12] M. Gold,[18] J. Gonzalez,[21] A. Gordon,[9] A. T. Goshaw,[6] K. Goulianos,[26] H. Grassmann,[6] A. Grewal,[21] L. Groer,[27] C. Grosso-Pilcher,[5] C. Haber,[14] S. R. Hahn,[7] R. Hamilton,[9]
Submitted to Physical Review Letters March 9, 1995.

R. Handler,[34] R. M. Hans,[35] K. Hara,[32] B. Harral,[21] R. M. Harris,[7] S. A. Hauger,[6] J. Hauser,[4] C. Hawk,[27] J. Heinrich,[21] D. Cronin-Hennessy,[6] R. Hollebeek,[21] L. Holloway,[10] A. Hölscher,[11] S. Hong,[16] G. Houk,[21] P. Hu,[22] B. T. Huffman,[22] R. Hughes,[25] P. Hurst,[9] J. Huston,[17] J. Huth,[9] J. Hylen,[7] M. Incagli,[23] J. Incandela,[7] H. Iso,[32] H. Jensen,[7] C. P. Jessop,[9] U. Joshi,[7] R. W. Kadel,[14] E. Kajfasz,[7a] T. Kamon,[30] T. Kaneko,[32] D. A. Kardelis,[10] H. Kasha,[35] Y. Kato,[19] L. Keeble,[8] R. D. Kennedy,[27] R. Kephart,[7] P. Kesten,[14] D. Kestenbaum,[9] R. M. Keup,[10] H. Keutelian,[7] F. Keyvan,[4] D. H. Kim,[7] H. S. Kim,[11] S. B. Kim,[16] S. H. Kim,[32] Y. K. Kim,[14] L. Kirsch,[3] P. Koehn,[25] K. Kondo,[32] J. Konigsberg,[9] S. Kopp,[5] K. Kordas,[11] W. Koska,[7] E. Kovacs,[7a] W. Kowald,[6] M. Krasberg,[16] J. Kroll,[7] M. Kruse,[24] S. E. Kuhlmann,[1] E. Kuns,[27] A. T. Laasanen,[24] N. Labanca,[23] S. Lammel,[4] J. I. Lamoureux,[3] T. LeCompte,[10] S. Leone,[23] J. D. Lewis,[7] P. Limon,[7] M. Lindgren,[4] T. M. Liss,[10] N. Lockyer,[21] C. Loomis,[27] O. Long,[21] M. Loreti,[20] E. H. Low,[21] J. Lu,[30] D. Lucchesi,[23] C. B. Luchini,[10] P. Lukens,[7] J. Lys,[14] P. Maas,[34] K. Maeshima,[7] A. Maghakian,[26] P. Maksimovic,[15] M. Mangano,[23] J. Mansour,[17] M. Mariotti,[20] J. P. Marriner,[7] A. Martin,[10] J. A. J. Matthews,[18] R. Mattingly,[15] P. McIntyre,[30] P. Melese,[26] A. Menzione,[23] E. Meschi,[23] G. Michail,[9] S. Mikamo,[13] M. Miller,[5] R. Miller,[17] T. Mimashi,[32] S. Miscetti,[8] M. Mishina,[13] H. Mitsushio,[32] S. Miyashita,[32] Y. Morita,[13] S. Moulding,[26] J. Mueller,[27] A. Mukherjee,[7] T. Muller,[4] P. Musgrave,[11] L. F. Nakae,[29] I. Nakano,[32] C. Nelson,[7] D. Neuberger,[4] C. Newman-Holmes,[7] L. Nodulman,[1] S. Ogawa,[32] S. H. Oh,[6] K. E. Ohl,[35] R. Oishi,[32] T. Okusawa,[19] C. Pagliarone,[23] R. Paoletti,[23] V. Papadimitriou,[31] S. Park,[7] J. Patrick,[7] G. Pauletta,[23] M. Paulini,[14] L. Pescara,[20] M. D. Peters,[14] T. J. Phillips,[6] G. Piacentino,[2] M. Pillai,[25] R. Plunkett,[7] L. Pondrom,[34] N. Produit,[14] J. Proudfoot,[1] F. Ptohos,[9] G. Punzi,[23] K. Ragan,[11] F. Rimondi,[2] L. Ristori,[23] M. Roach-Bellino,[33] W. J. Robertson,[6] T. Rodrigo,[7] J. Romano,[5] L. Rosenson,[15] W. K. Sakumoto,[25] D. Saltzberg,[5] A. Sansoni,[8] V. Scarpine,[30] A. Schindler,[14] P. Schlabach,[9] E. E. Schmidt,[7] M. P. Schmidt,[35] O. Schneider,[14] G. F. Sciacca,[23] A. Scribano,[23] S. Segler,[7] S. Seidel,[18] Y. Seiya,[32] G. Sganos,[11] A. Sgolacchia,[2] M. Shapiro,[14] N. M. Shaw,[24] Q. Shen,[24] P. F. Shepard,[22] M. Shimojima,[32] M. Shochet,[5] J. Siegrist,[29] A. Sill,[31] P. Sinervo,[11] P. Singh,[22] J. Skarha,[12] K. Sliwa,[33] D. A. Smith,[23] F. D. Snider,[12] L. Song,[7] T. Song,[16] J. Spalding,[7] L. Spiegel,[7] P. Sphicas,[15] A. Spies,[12] L. Stanco,[20] J. Steele,[34] A. Stefanini,[23] K. Strahl,[11] J. Strait,[7] D. Stuart,[7] G. Sullivan,[5] K. Sumorok,[15] R. L. Swartz, Jr.,[10] T. Takahashi,[19] K. Takikawa,[32] F. Tartarelli,[23] W. Taylor,[11] P. K. Teng,[28] Y. Teramoto,[19] S. Tether,[15] D. Theriot,[7] J. Thomas,[29] T. L. Thomas,[18] R. Thun,[16] M. Timko,[33] P. Tipton,[25] A. Titov,[26] S. Tkaczyk,[7] K. Tollefson,[25]

A. Tollestrup,[7] J. Tonnison,[24] J. F. de Troconiz,[9] J. Tseng,[12] M. Turcotte,[29] N. Turini,[23] N. Uemura,[32] F. Ukegawa,[21] G. Unal,[21] S. C. van den Brink,[22] S. Vejcik, III,[16] R. Vidal,[7] M. Vondracek,[10] R. G. Wagner,[1] R. L. Wagner,[7] N. Wainer,[7] R. C. Walker,[25] C. H. Wang,[28] G. Wang,[23] J. Wang,[5] M. J. Wang,[28] Q. F. Wang,[26] A. Warburton,[11] G. Watts,[25] T. Watts,[27] R. Webb,[30] C. Wendt,[34] H. Wenzel,[14] W. C. Wester, III,[14] T. Westhusing,[10] A. B. Wicklund,[1] E. Wicklund,[7] R. Wilkinson,[21] H. H. Williams,[21] P. Wilson,[5] B. L. Winer,[25] J. Wolinski,[30] D. Y. Wu,[16] X. Wu,[23] J. Wyss,[20] A. Yagil,[7] W. Yao,[14] K. Yasuoka,[32] Y. Ye,[11] G. P. Yeh,[7] P. Yeh,[28] M. Yin,[6] J. Yoh,[7] T. Yoshida,[19] D. Yovanovitch,[7] I. Yu,[35] J. C. Yun,[7] A. Zanetti,[23] F. Zetti,[23] L. Zhang,[34] S. Zhang,[16] W. Zhang,[21] and S. Zucchelli[2]

(CDF Collaboration)

[1] *Argonne National Laboratory, Argonne, Illinois 60439*

[2] *Istituto Nazionale di Fisica Nucleare, University of Bologna, I-40126 Bologna, Italy*

[3] *Brandeis University, Waltham, Massachusetts 02254*

[4] *University of California at Los Angeles, Los Angeles, California 90024*

[5] *University of Chicago, Chicago, Illinois 60637*

[6] *Duke University, Durham, North Carolina 27708*

[7] *Fermi National Accelerator Laboratory, Batavia, Illinois 60510*

[8] *Laboratori Nazionali di Frascati, Istituto Nazionale di Fisica Nucleare, I-00044 Frascati, Italy*

[9] *Harvard University, Cambridge, Massachusetts 02138*

[10] *University of Illinois, Urbana, Illinois 61801*

[11] *Institute of Particle Physics, McGill University, Montreal H3A 2T8, and University of Toronto, Toronto M5S 1A7, Canada*

[12] *The Johns Hopkins University, Baltimore, Maryland 21218*

[13] *National Laboratory for High Energy Physics (KEK), Tsukuba, Ibaraki 305, Japan*

[14] *Lawrence Berkeley Laboratory, Berkeley, California 94720*

[15] *Massachusetts Institute of Technology, Cambridge, Massachusetts 02139*

[16] *University of Michigan, Ann Arbor, Michigan 48109*

[17] *Michigan State University, East Lansing, Michigan 48824*

[18] *University of New Mexico, Albuquerque, New Mexico 87131*

[19] *Osaka City University, Osaka 588, Japan*

[20] *Universita di Padova, Instituto Nazionale di Fisica Nucleare, Sezione di Padova, I-35131 Padova, Italy*

[21] *University of Pennsylvania, Philadelphia, Pennsylvania 19104*

[22] *University of Pittsburgh, Pittsburgh, Pennsylvania 15260*

[23] *Istituto Nazionale di Fisica Nucleare, University and Scuola Normale Superiore of Pisa, I-56100 Pisa, Italy*

[24] *Purdue University, West Lafayette, Indiana 47907*

[25] *University of Rochester, Rochester, New York 14627*

[26] *Rockefeller University, New York, New York 10021*

[27] *Rutgers University, Piscataway, New Jersey 08854*

[28] *Academia Sinica, Taiwan 11529, Republic of China*

[29] *Superconducting Super Collider Laboratory, Dallas, Texas 75237*

[30] *Texas A&M University, College Station, Texas 77843*

[31] *Texas Tech University, Lubbock, Texas 79409*

[32] *University of Tsukuba, Tsukuba, Ibaraki 305, Japan*

[33] *Tufts University, Medford, Massachusetts 02155*

[34] *University of Wisconsin, Madison, Wisconsin 53706*

[35] *Yale University, New Haven, Connecticut 06511*

PACS numbers: 13.87Ce,12.38Qk

Abstract

The properties of two-, three-, four-, five-, and six-jet events with multijet masses > 600 GeV/c^2 are compared with QCD predictions. The shapes of the multijet-mass and leading-jet-angular distributions are approximately independent of jet multiplicity and are well described by the NJETS matrix element calculation and the HERWIG parton shower Monte Carlo predictions. The observed jet transverse momentum distributions for three- and four-jet events discriminate between the matrix element and parton shower predictions, the data favoring the matrix element calculation.

In this paper we describe the properties of multijet events with multijet masses m $>$ 600 GeV/c^2 recorded in proton-antiproton collisions at a center-of-mass energy of 1.8 TeV. The data were recorded by the CDF experiment at the Fermilab Tevatron collider over the period 1992 - 1994, and correspond to an integrated luminosity of 35 pb^{-1}.

Within the framework of perturbative QCD, multijet events are expected to arise from hard parton-parton scattering. The outgoing scattered partons manifest themselves as hadronic jets. The lowest order QCD diagrams predict two jets in the final state. Higher order corrections can give rise to events with more than two jets. A comparison of the properties of multijet events with QCD predictions provides a test of the higher-order QCD corrections, and enables a search for new phenomena associated with the presence of many hard partons in the final state.

In a previous analysis [1] based on a 4 pb^{-1} data sample we showed that a good first description of multijet events at high mass was provided by the HERWIG [2] QCD parton shower Monte Carlo program interfaced to a full simulation of the CDF detector response. The HERWIG calculation includes initial- and final-state gluon radiation, color coherence, hadronization, and an underlying event accompanying the hard scattering. In the present paper we compare a much larger data sample with predictions from (i) the HERWIG Monte Carlo program, and (ii) the NJETS [3] complete leading order (LO) QCD matrix element Monte Carlo program for $2 \rightarrow N$ scattering. Note that the NJETS calculation has been used to provide predictions for topologies with up to five final-state jets. This comparison enables us to further test the QCD predictions, and see if the data discriminate between the complete LO matrix element predictions and the parton-shower Monte Carlo approximation.

A full description of the CDF detector can be found in ref. [4]. The analysis described in this paper exploits the CDF calorimeters, which cover the pseudorapidity region $|\eta| < 4.2$, where $|\eta| \equiv -\ln(\tan\theta/2)$. The calorimeters are constructed in a tower geometry in η - ϕ (azimuthal angle) space. The towers are 0.1 units wide in η. The tower widths in ϕ are 15° in the central region and 5° at larger η (approximately $|\eta| > 1.2$). Jets are reconstructed using an algorithm that forms clusters from localized energy depositions in the calorimeter towers. Calorimeter towers are associated with a jet if their separation from the jet axis in (η, ϕ)-space $\Delta R = (\Delta\eta^2 + \Delta\phi^2)^{1/2} < R_0$. For the analysis described in this paper the clustering cone radius was chosen to be $R_0 = 0.7$. With this R_0 a plot of the separation between all jets observed in the data sample described below reveals that to a good approximation clusters with separations $\Delta R < 0.8$ are always merged by the jet algorithm

into a single jet, and clusters with separations $\Delta R > 1.0$ are never merged. Thus, the effective minimum observable separation between jets $\Delta R_{MIN} = 0.9 \pm 0.1$. Jet energies are corrected for calorimeter non-linearities, energy lost in uninstrumented regions and outside of the clustering cone, and energy gained from the underlying event. The jet corrections typically increase jet energies by 25% for jets with transverse energy $E_T = E \sin\theta > 60$ GeV, where θ is the angle between the jet axis and the beam direction. The jet corrections are larger for lower E_T jets, and typically increase jet energies by about 30% (40%) for jets with $E_T = 40$ GeV (20 GeV). After correction, jet energies are measured with a precision σ_E/E of approximately 0.1 and multijet masses calculated from the jet four-vectors are measured with a precision σ_m/m of approximately 0.1. The systematic uncertainty on the jet energy scale is 5%. Full details of the CDF jet algorithm, jet corrections, and jet resolution functions can be found in ref. [5].

The data were recorded using a trigger which required $\sum E_T > 300$ GeV, where the sum is over all uncorrected jets with transverse energy $E_T > 10$ GeV, and the calculation was done assuming an event vertex at the center of the detector. In the subsequent analysis the $\sum E_T$ was recalculated using the reconstructed vertex position and corrected jet energies, and summing over all jets with corrected $E_T > 20$ GeV. The resulting $\sum E_T$ distribution peaks at 400 GeV. At lower $\sum E_T$ the trigger requirements are no longer fully efficient. Events were retained with $\sum E_T > 420$ GeV. To reject backgrounds from cosmic ray interactions, beam halo, and detector malfunctions, the events were required to have (i) total energy less than 2000 GeV, (ii) a primary vertex reconstructed within 60 cm of the detector center, (iii) no significant energy deposited in the hadron calorimeters out-of-time with the proton-antiproton collision, and (iv) missing-E_T ($\not\!\!E_T$) significance [1] $S \equiv \not\!\!E_T / (\sum E_T)^{1/2} < 6$. These requirements select 9980 multijet events, of which 4072 events have multijet masses m > 600 GeV/c^2. Finally we have applied cuts on the values of multijet mass and leading-jet scattering angle. To motivate these mass and angular requirements consider a two-jet event in which the two-jet system is at rest in the laboratory frame. The $\sum E_T > 420$ GeV requirement places a mass dependent restriction on the two-jet center-of-mass scattering angle θ^* such that $|\cos\theta^*| < (1 - (420/m)^2)^{1/2}$, where m is in units of GeV/c^2. To obtain an acceptance which is independent of mass above a minimum mass m_0 we must restrict ourselves to the angular region $|\cos\theta^*| < \cos\theta_{MAX}$, and choose a value for $\cos\theta_{MAX}$ less than $(1 - (420/m_0)^2)^{1/2}$. In the present analysis we have chosen $m_0 = 600$ GeV/c^2, $\cos\theta_{MAX} = 2/3$, and applied the angular cut to the leading (highest E_T) jet in the multijet rest-frame.

This selects 1874 events, of which 345 have 2 jets with $E_T > 20$ GeV, 612 have 3 jets, 554 have 4 jets, 250 have 5 jets, 88 have 6 jets, 21 have 7 jets, 4 have 8 jets, and there are no events with more than 8 jets.

The multijet mass distributions for events with $|\cos\theta^*| < 2/3$ are shown in Fig. 1 for 2-jet, 3-jet, 4-jet, 5-jet, and 6-jet events, with no requirement on the minimum multijet masses. The mass distributions extend up to masses of about 1 TeV/c^2. As expected, the mass distributions exhibit a turn-over near to 600 GeV/c^2. At lower masses the $\sum E_T$ requirement is more restrictive than the angular cut, and results in a decreasing angular acceptance with decreasing multijet mass. To check that the shapes of the mass distributions are not sensitive to the uncertainty on the jet energy scale, we have increased and decreased the jet energy scale by $\pm 1\sigma$ and repeated the analysis. The resulting small changes in the shapes of the multijet mass distributions are smaller than or comparable to the statistical uncertainties on the measurements. The HERWIG Monte Carlo predictions are in reasonable agreement with all of the multijet mass distributions. Note that the HERWIG predictions include a full simulation of the CDF detector response, and use the CTEQ1M structure functions [6] with the scale given by $Q^2 = stu/2(s^2 + u^2 + t^2)$, where s, t, and u are the Mandelstam variables. This Q^2 is approximately equal to the square of the average E_T of the outgoing scattered partons. The predictions from the LO QCD matrix element Monte Carlo program NJETS are also shown in Fig. 1 for all but the 6-jet distribution. On each distribution there are 8 NJETS curves corresponding to the structure function, Q^2 scale, and ΔR_{MIN} choices summarized in Table 1. The NJETS calculation does not include a full simulation of the CDF detector, but does include a gaussian jet energy resolution function with $\sigma_E/\mathrm{E} = 0.1$. The resulting predictions give reasonable descriptions of the shapes of the measured mass distributions. Furthermore, compared to the statistical precision of the measurements, the NJETS predictions for the shapes of the mass distributions are not sensitive to uncertainties associated with the choice of structure function, Q^2 scale, or ΔR_{MIN}.

Above the turn-on, all of the multijet mass distributions have similar shapes. This is seen clearly in Fig. 2 which shows the 3-jet/2-jet, 4-jet/2-jet, 5-jet/2-jet, and 6-jet/2-jet ratios as a function of multijet mass. These ratios are almost independent of mass. Within the substantial theoretical uncertainties which are associated predominantly with the choice of Q^2-scale, both the parton shower Monte Carlo predictions and the complete LO QCD matrix element predictions give a good description of the mass dependent multijet ratios, and therefore give a reasonable description of the observed jet multiplicity distribution.

The ability of the parton shower Monte Carlo predictions to describe the multijet-mass and jet-multiplicity distributions suggests that $2 \rightarrow 2$ scattering plus gluon radiation provides a good approximate description of the production of events with several jets in the final state. In this picture we would expect the leading-jet angular distributions to be similar to the two-jet angular distribution, even when there are many final-state jets. This is indeed seen to be the case in Fig. 3 which shows that for events with $m > 600$ GeV/c^2, the leading-jet angular distributions are similar to the Rutherford scattering form independent of jet multiplicity, and are well described by both the HERWIG and NJETS QCD predictions.

At some level, we would expect to see differences between the HERWIG and NJETS predictions which reflect the presence of additional LO QCD diagrams in the NJETS matrix element calculation. Differences are indeed observed in the inclusive jet transverse-momentum (p_T) distributions, shown in Fig. 4 for the different multijet topologies. The 2-jet, 3-jet, 4-jet, and 5-jet inclusive-jet p_T distributions exhibit a peak in the region 200 - 300 GeV/c, reflecting the effect of the $\sum E_T$ requirement on events in which most of the $\sum E_T$ is associated with two hard jets in the final state. The observed jet p_T distributions are well described by the NJETS predictions. Within the statistical precision of the data, the HERWIG predictions also give a reasonable description of the 2-jet, 5-jet, and 6-jet distributions. However for 3-jet and 4-jet events the HERWIG predictions overestimate the jet rate at intermediate p_T between the two-jet dominance peak at high-p_T and the soft gluon enhancement at low-p_T.

In summary, the properties of multijet events with multijet mass $m > 600$ GeV/c^2 and up to six jets in the final state have been compared with QCD predictions. The jet multiplicity distribution is well described by both a complete LO matrix element calculation (NJETS) and a parton shower Monte Carlo calculation (HERWIG). The shapes of the multijet-mass and leading-jet angular distributions are approximately independent of jet multiplicity, and are well described by both HERWIG and NJETS. This suggests that $2 \rightarrow 2$ scattering plus gluon radiation provides a good approximate description of the production of events with several jets in the final state. However, the observed inclusive-jet p_T distributions for 3-jet and 4-jet events do discriminate between the NJETS and HERWIG predictions. The parton-shower Monte Carlo program predicts too many jets at intermediate transverse momenta.

We thank the Fermilab Accelerator Division and the technical and support staff of our respective institutions. We also acknowledge the assistance of Walter Giele in producing

the NJETS Monte Carlo predictions. This work was supported by the U.S. Department of Energy, the U.S. National Science Foundation, the Istituto Nazionale di Fisica Nucleare of Italy, the Ministry of Science, Culture and Education of Japan, the Natural Sciences and Engineering Research Council of Canada, and the A.P. Sloan Foundation.

References

[1] F. Abe et al. (CDF Collaboration), *Phys. Rev.* **D45**, 2249 (1992).

[2] G. Marchesini and B. Webber, *Nucl. Phys.* **B310**, 461 (1988).

[3] F.A. Berends and H. Kuijf, *Nucl. Phys.* **B353**, 59 (1991).

[4] F. Abe et al. (CDF Collaboration), *Nucl. Instr. and Meth.* **A271**, 387 (1988).

[5] F. Abe et al. (CDF Collaboration), *Phys. Rev.* **D45**, 1448 (1992).

[6] H.L. Lai et al; Preprint MSU-HEP-41024, CTEQ-404, (to be published).

[7] A.D. Martin, R.G. Roberts, W.J. Stirling; *Phys. Lett.* **B306**, 145 (1993).

Structure Function	$Q^2 - Scale$	ΔR_{MIN}
KMRSD−	$< p_T >^2$	0.8
KMRSD−	$< p_T >^2$	0.9
KMRSD−	m^2	0.9
KMRSD−	$< p_T >^2$	1.0
KMRSS0	$< p_T >^2$	0.9
KMRSD0	$< p_T >^2$	0.9
CTEQ1M	$< p_T >^2$	0.9
CTEQ1MS	$< p_T >^2$	0.9

Table 1: Parameter choices used for the 8 NJETS calculations. The structure function choices are described in refs. [6] and [7].

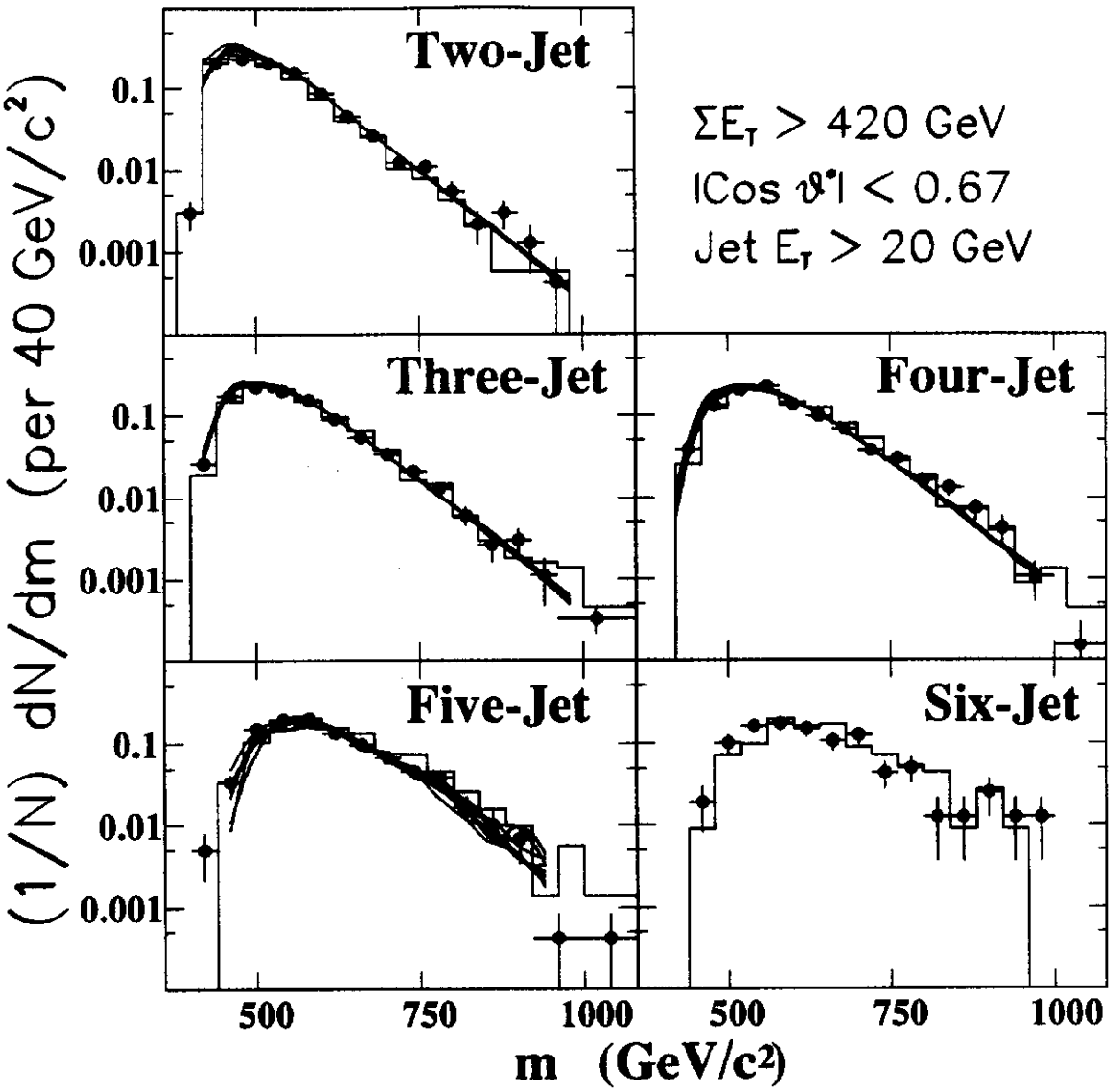

Figure 1: Exclusive multijet mass distributions. The data (solid points) are compared with HERWIG predictions (histogram) and NJETS predictions for the eight parameter choices listed in Table 1 (curves).

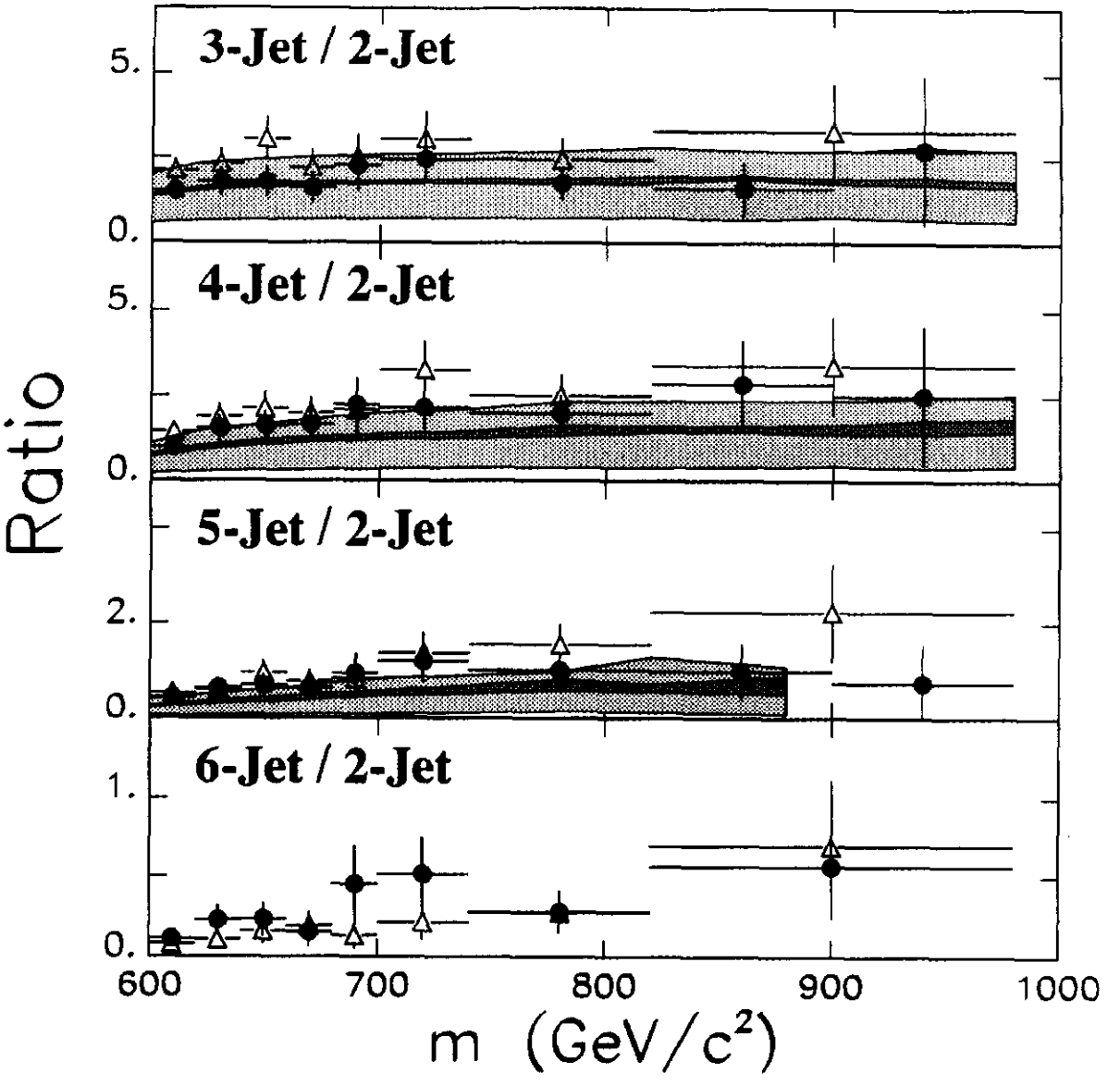

Figure 2: Exclusive Multijet mass distributions divided by the corresponding two-jet distribution. The data (solid points) are compared with HERWIG predictions (triangles) and NJETS predictions (bands). The inner band shows the variation of the NJETS prediction with choice of structure function listed in Table 1, and a Q^2 scale of $< p_T >^2$. The outer band shows the variation of the predictions with choice of Q^2-scale listed in Table 1. The variation with ΔR_{MIN} is negligible.

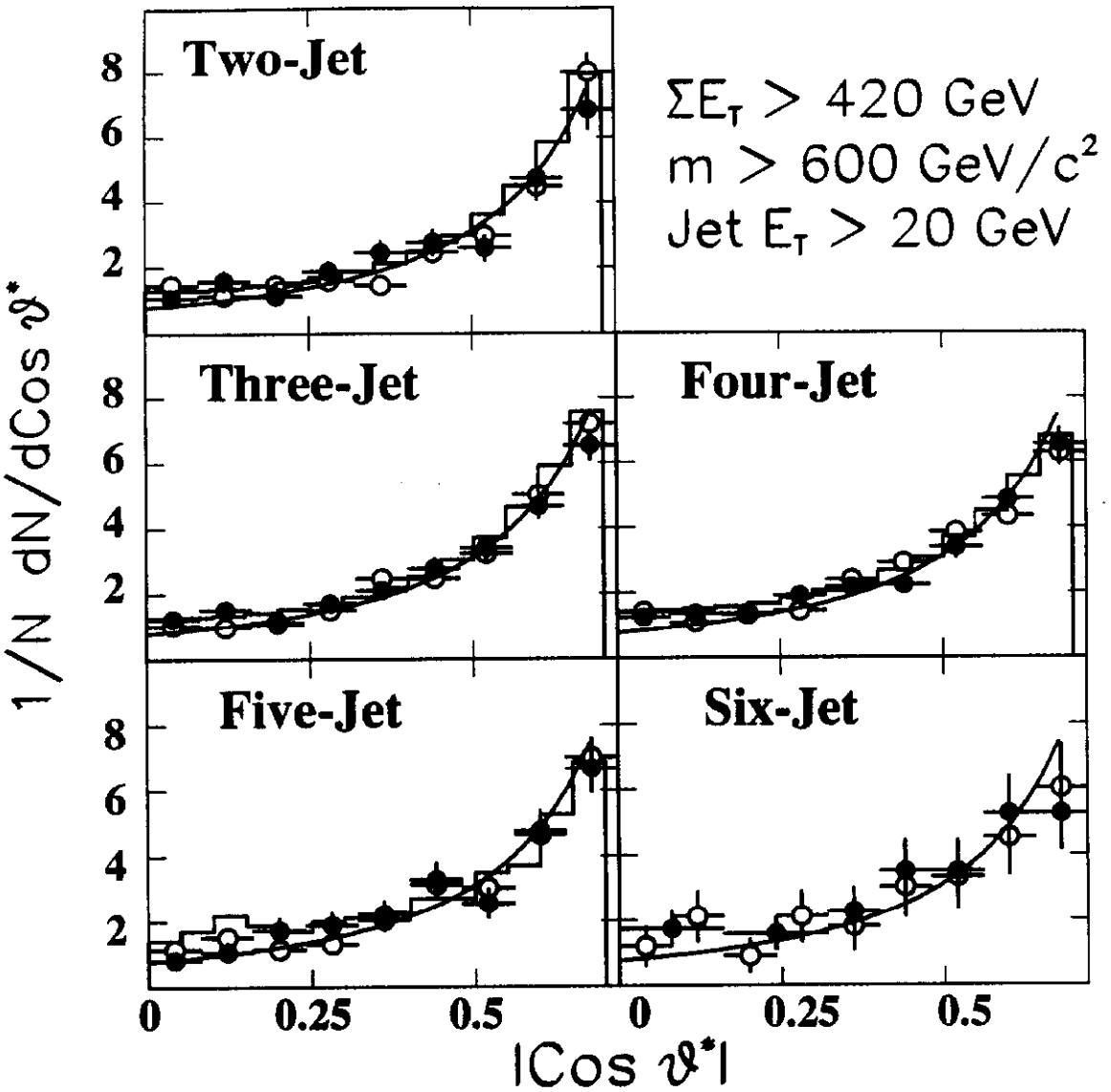

Figure 3: Leading-jet angular distributions. The data (solid points) are compared with HERWIG predictions (open points) and NJETS predictions (histograms). The curves show the Rutherford scattering form $(1 - \cos\theta^*)^{-2}$.

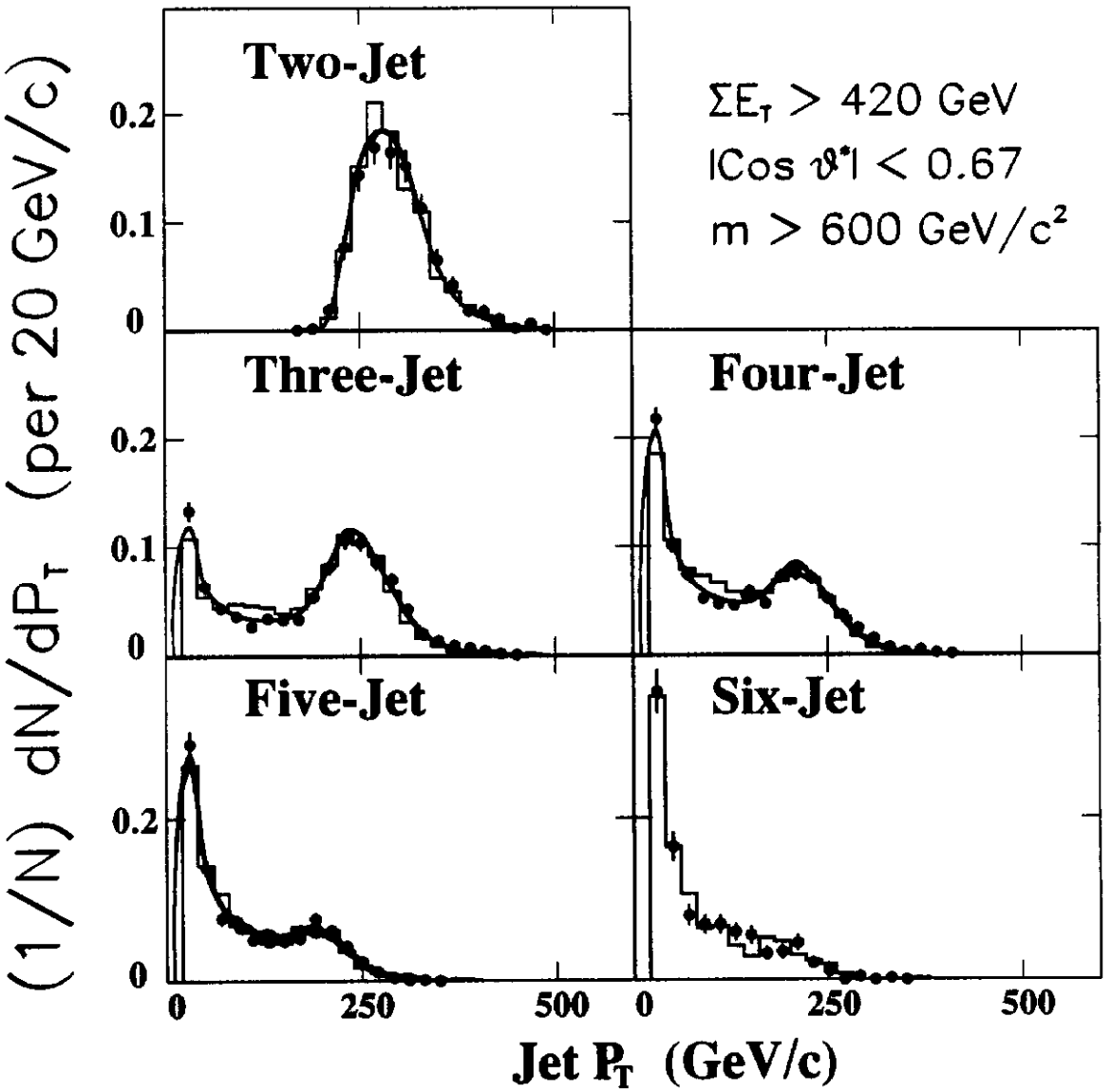

Figure 4: Jet transverse momentum distributions.The data (solid points) are compared with HERWIG predictions (histogram) and NJETS predictions for the eight parameter choices listed in Table 1 (curves).